Design and Cost Review of 2 m² Heliostat Prototypes

James Larmuth[1], Karel Malan[2], Paul Gauché[3]

[1] Solar Thermal Energy Research Group (STERG), Dept. Mechanical and Mechatronic Engineering, Stellenbosch University, Stellenbosch, South Africa +27 (0) 83 654 3401; larmuth@sun.ac.za

[2] Solar Thermal Energy Research Group (STERG); karel@sun.ac.za

[3] Sr. Researcher and Director of the Solar Thermal Energy Research Group (STERG), paulgauche@sun.ac.za

Abstract

The Solar Thermal Energy Research Group (STERG) is currently upgrading its solar roof laboratory at the University of Stellenbosch by the addition of an internally developed 40 m² (aperture) heliostat test facility. Practical learning gained from heliostat prototype development is presented. This paper presents a design and cost review of two 2 m² heliostat prototypes incorporating different tracking mechanisms and provides insight into low volume heliostat costs.

Key words: Heliostats; CSP; Practical Challenges; Heliostat Cost; Helio-40

1 Introduction

The Solar Thermal Energy Research Group (STERG) of the University of Stellenbosch is currently the largest solar thermal research group in Southern Africa. STERG's research structure is built around strategically selected technologies, the primary technology being a concept called the SUNSPOT cycle [1]. The SUNSPOT cycle is a CSP concept that incorporates an asynchronous combined cycle central receiver system. This concept forms a convenient platform for arranging R&D as it can be broken into generic components that would also be compatible with less complicated receiver technologies.

In order to aid further research, a grant for special equipment has been provided by SASOL; this grant allows for the implementation of a 40 m² (field aperture) heliostat test facility on the open air solar roof laboratory of the department of mechanical and mechatronic engineering. The project was named Helio-40 and formed an intermediate scale up of an existing 1.62 m² heliostat array consisting of 18 heliostats.

The solar roof laboratory is a 500 m² open air facility with a control room as well as an 18 m multipurpose lattice tower, which is to be integrated into the Helio-40 project. Helio-40 proposal layout consisted of fourteen heliostats to be located on the roof of the control room with a further six heliostats fixed to a floor mounted lattice pedestal (see Fig.1.).

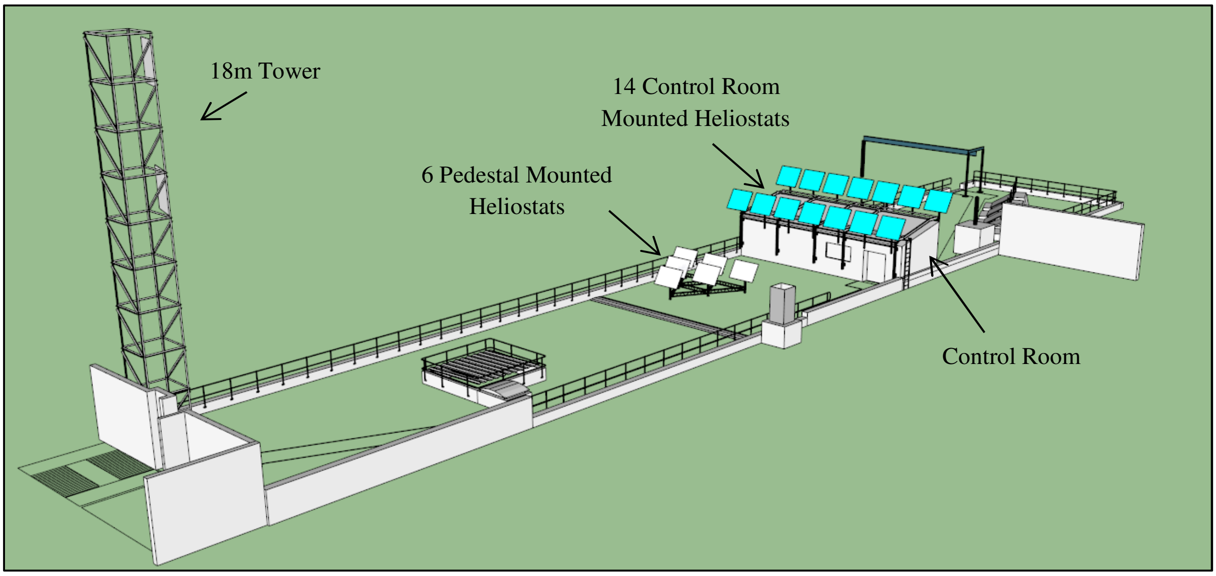

Fig. 1. Conceptual model of the solar roof laboratory fitted with 40 m² of heliostat aperture

The project was allocated a 12 month delivery schedule and listed its performance and safety priorities above cost. These priorities as well as the location of the heliostat test facility on the roof of a university building provided a unique challenge set to the heliostat prototype development, as the resulting safety and wind loading requirements differ significantly from that of a conventional field based heliostat facility. The high level Helio-40 requirements are shown in Table 1.

No.	Requirement	Minimum Requirement Value
1	Total aperture area	30 m^2
2	On-target accuracy	1.875 mrad normal vector error (sum of component Error) 150 mm deviation on target at a 40 m slant range
3	Component accuracy	0.625 mrad RMS tracking error 0.625 mrad pedestal flex 0.625 mrad mechanism flex
4	Operational winds	Track up 20 km/h Stow between 20 km/h and 50 km/h
5	Survival Wind Loads	Survive stow loads of up to 100 km/h
6	Reflector Image	Image minimized for 14:00 – 16:00 experiments to have >75% of reflected energy falling within focused image area on target.
7	Flexibility	Modular Design: swappable heliostat facets, drives and pylons
8	Facet	2 m^2 square facets with demountable connection points.
9	Support structure (headstock): interface between drive and mirror	Universal facet connection point, thereby allowing for interchangeable facets and tracking mechanisms
10	Foundation	Floor standing steelwork lattice pedestal to meet component accuracy specifications. Control room roof structure to meet pedestal accuracy specifications.
11	Tracking mechanism	Default pedestal with either azimuth elevation tracking or fixed horizontal
12	Array layout	2/3 of aperture installed on control room roof and 1/3 of aperture positioned on lab floor
13	Cost	430 000 ZAR
14	System Life Span	5 Years

Table 1. Helio-40 high level heliostat requirements

2 Heliostat Design Overview

2.1 Wind Loading

In order to design an optimal heliostat, accurate design wind loads are required [2]. The Helio-40 heliostats are required to track during wind speeds within an operational threshold, move to stow position within a movement threshold and survive maximum wind speeds in the stow position. Helio-40's location on the solar roof laboratory is surrounded by larger buildings in all directions, making the prediction of atmospheric wind loading difficult when compared to methods for conventional systems in open fields. Therefore, it was the intention of the design team to obtain a set of worst case load inputs in order to best dimension the heliostat prototypes for safe operation. The heliostats were not required to be cost optimised and therefore it was understood that large safety factors will be incorporated into these wind loads. This would ensure that the test facilities safety and optical performance is prioritised.

In order to set the operational wind speed requirements (as shown in Table 1), wind measurement data obtained from an anemometer located on the North East, adjacent roof was used. The anemometer yielded per minute, time averaged (TA) data for an entire year. Although the resolution did not allow for the identification of peak gusts, mean wind speeds could be obtained. The maximum TA value recorded in 2012 was 37 km/h and the yearly average was 9 km/h. Based on this data a maximum tracking windspeed threshold of 20 km/h was selected and a survival wind speed of 100 km/h (in the stow position). The 20 km/h threshold allows for standard tracking operation for the majority of the year. When the heliostats are in operation and wind speeds exceed the 20 km/h threshold a control system linked to a high resolution anemometer (reading 2-3 sec data) will trigger the heliostats to stow within 3 minutes.

Experimental wind tunnel data published by Peterka & Derickson [2], allowed for the calculation of worst case wind force and moment values about the X, Y and Z heliostat axes (Fig. 2. - left). The published force and drag coefficients presested by Peterka & Derickson [2] are for an an isoloated heliostat with an aspect ratio of 1 (Fig. 2. right).

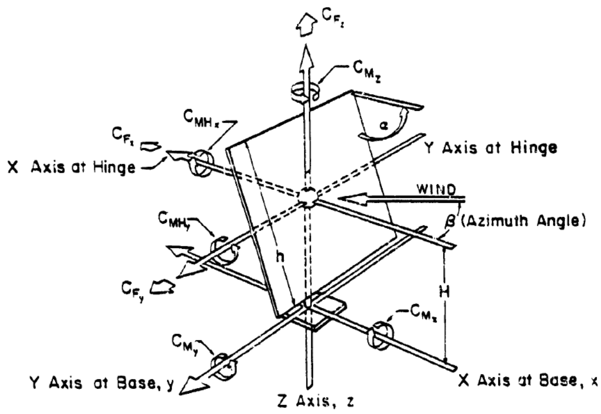

	Fx, My Max	Fz, MHy Max	Mz Max	Stow Loads
PEAK LOADS				
α, degrees	90	30	90	0
β, degrees	0	0	65	0
Fx	4.0	2.1	3.7	0.6
Fz	1.0	2.8	0.5	0.9
MHy	0.25	0.6	0.15	0.2
Mz	0.29	0.06	0.7	0.02
MEAN LOADS				
α, degrees	90	30	90	0
β, degrees	0	0	65	0
Fx	2.0	1.0	1.6	0.1
Fz	0.3	1.35	0.3	0.1
MHy	0.02	0.25	0.02	0.02
Mz	0	0	0.25	0

n = 0.15   Tu = 18%   Zo = 0.03 meters

Fig. 2.: Coordinate system for heliostat (Left); Published wind load coefficients (Right) **[2]**

Calculated load	Load definition	Worst case load: rounded up
F_x: Horizontal wind force perpendicular to elevation shaft	$F_x = C_{FX}\frac{\rho}{2}V^2A$	150 N (Vertical facet α = 90°)
F_z: Vertical wind force	$F_z = C_{FZ}\frac{\rho}{2}V^2A$	110 N (Elevated facet α = 30°)
M_{hy}: Elevation Moment	$M_{YH} = C_{M_{hy}}\frac{\rho}{2}V^2Ah$	40 Nm
M_Z: Azimuthal Moment	$M_z = C_{M_z}\frac{\rho}{2}V^2Ah$	40 Nm
M_y: Base overturning moment	$M_Y = C_{M_Y}\frac{\rho}{2}V^2AH$	320 Nm

Table 2. Calculated wind loads using Peterka and Derickson [2]

2.2 2 m^2 Heliostat Prototypes

Heliostats require two orthogonal degrees of freedom in order to continuously reflect solar irradiance onto a receiver or target. The heliostat tracking mechanism describes the orientation of these two degrees of freedom. Two single Helio-40 prototypes were developed in parallel prior to deciding on a final Helio-40 design (see Fig. 3.). As per the flexibility requirements (Item 7; Table 1) both prototypes have identical facets and pylons but incorporate different tracking mechanisms and drive configurations. The first prototype incorporates a fixed horizontal (FH) tracking mechanism while the second uses an azimuth elevation (AE) tracking mechanism. A target aligned tracking mechanism was also reviewed in the early project stages but despite its superior optical performance [3] was excluded due to it requiring accurate installation and alignment.

Due to the project priority structure, neither prototypes were optimised for structural performance, and both designs use standard off-the-shelf steel cross sections, bearings and drives. In addition, large safety factors were used to account for low wind loading confidence, as well as the high stiffness resulting from the acute on target accuracy requirements. When dimensioning the heliostat structures it was found that the section sizes and beam quality resulting from the 0.625 mrad structural deflection requirements and operational wind loads far exceeded those obtained from the survival requirements.

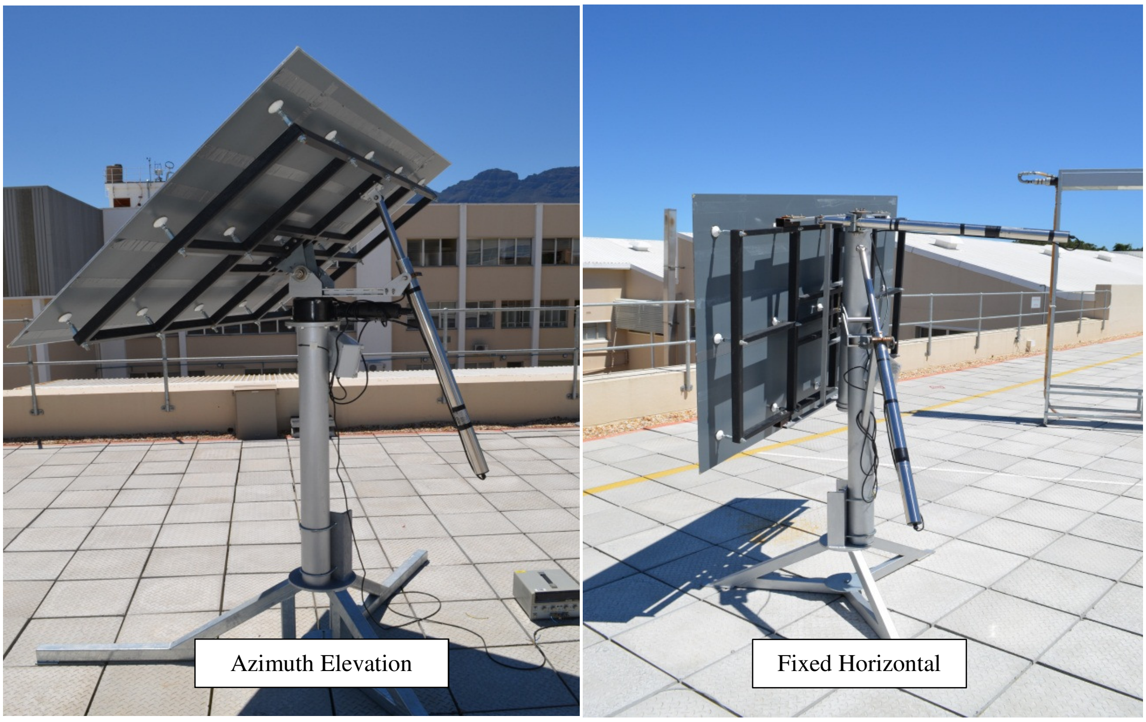

Fig. 3. First generation Helio-40 prototypes – fitted with early facet concept

2.2.1 Tracking Mechanisms

In an AE configuration the primary rotational axis (ground mounted axis) rotates around a vertical axis while the secondary axis rotates around the horizontal (see Figure 4). This arrangement typically operates with two orthogonal rotary drives or a combination of a rotary drive and a linear actuator, the latter is used in Helio-40. This configuration has the advantage of a 360° azimuth displacement as well as a constant azimuth holding torque at any displacement position. A disadvantage is that it's three dimensional rotation requires larger centre-to-centre distances in order to avoid heliostat collision [4] [5] and therefore experiences lower packing ratios (see Figure: 4- C).

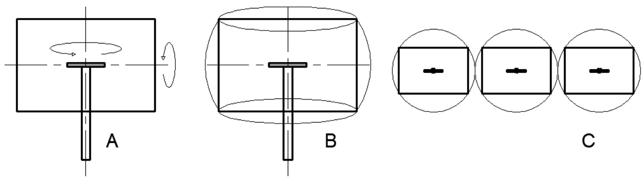

Fig. 4. Azimuth elevation clearance requirements adapted from Schramek and Mills [4]

The FH configuration fixes the vertical primary axis and allows rotational movement in the horizontal direction by means of an off-set secondary axis. This arrangement allows for easy integration with linear drives as well as reduced collision and improved packing ratios (see Figure 5-C) [5]. This mechanism is disadvantaged by the non-constant holding force of the linear actuator, which are smaller when the heliostat facet is in its maximum displacement position.

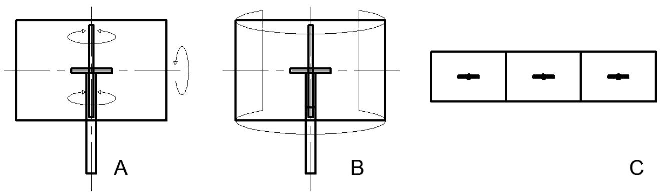

Fig. 5. Fixed horizontal tracking mechanism adapted from Cordes [5]

2.2.2 Drives

An off-the-shelf, slewing drive and planetary gearbox with a combined reduction ratio of 35 650:1 was used for the azimuth drive in the AE tracking mechanism. The slew drive specifications indicated a holding torque of 250 Nm, and a 0° tracking accuracy (zero backlash). Based on a review of several other suppliers the smallest slew drive seen to be available during the project schedule was a three inch slew drive. This drive selection resulted in an overdesign as the slew selected is able to handle facets up to 5 m^2. Despite the supplier's published backlash specifications, initial open loop tests showed the slew drive to have backlash of 0.6 as soon as a moment load above 10 Nm was applied. To overcome this, a prototype pre-load mechanism was constructed to remove the backlash.

The linear actuators selected have a stroke length of 520 mm and are able to operate at up to 1000N (dynamic load) and to handle a Static load of up to 3400 N. The selection was based on a required stroke length of 500 mm on the FH prototype in order to move the facets secondary axis through 100° without compromising the mechanisms holding force in the maximum displacement position. For consistency and continued modular flexibility these actuators were selected as the default actuators for both mechanisms. Similar to that of the slew drive these actuators are capable of driving larger facets. Suppliers of smaller more applicable linear actuators have been sourced and future tests aim to explore the use of smaller drives on the Helio-40 heliostats.

2.2.3 Facet

In the early project stages a square 1414mm×1414 mm (2.0 m^2) facet was envisioned, this facet size and aspect ratio was later changed to a standard glass sheet size of 1830x1220mm (2.2 m^2).

The default facet assembly was constructed using mirror sheet bonded to a mild steel rectangular tubing backing. A mandrel was machined to form a positive spherical shape for a focal length of 47.5m. The mirror sheet was then placed onto the mandrel where it conformed to the mandrel shape under gravity. Once resting in place the galvanised backing frame was bonded in place using combination of resin and foam batting filler.

2.2.4 Safety

The heliostat focal length was set to 47.5 m; at this range permanent retinal damage can be caused if a person intercepts the beam near its focal point [6]. Certain emergency situations may require the heliostats to stow in an entirely south facing direction to avoid uncontrolled reflection in the event of control failure or during initial installation and testing. Furthermore adaptions to the facet were put in place which allows for removable facet covers with small holes in the centre. These covers reduce the facet aperture by 95 % and still allow for initial tracking tests to be carried out. In addition, special purpose covers on the side of the roof will ensure that no stray reflections can reach the surrounding buildings.

3 Heliostat Cost Review

Heliostats form approximately 40% of the total plant costs of commercial central receiver systems [7]. Due to the large quantity of heliostats required in a solar field, a small cost improvement on a single heliostat design can significantly reduce LCOE.

3.1 Heliostat Weight Analysis

A heliostat is typically a high volume product. In terms of products manufactured under high production rates the product mass generally indicates some degree of its cost [8] [9]. The specific mass values for the AE and FH mechanisms are 78 kg and 75 kg respectively. Several glass metal heliostat specifications in the public domain show that existing heliostat structures have masses between 30 kg/m^2 and 60 kg/m^2 excluding foundations [10]. The AZ and FH, Helio-40 prototypes presented have respective masses of 35 kg/m^2 and 34 kg/m^2, thereby showing proportion to the lower end of the conventional glass metal design masses without considering heliostat scale. The respective component weights as well as the percentages of commodity used to build and assemble each of the Helio-40 prototypes are shown in Fig. 6.

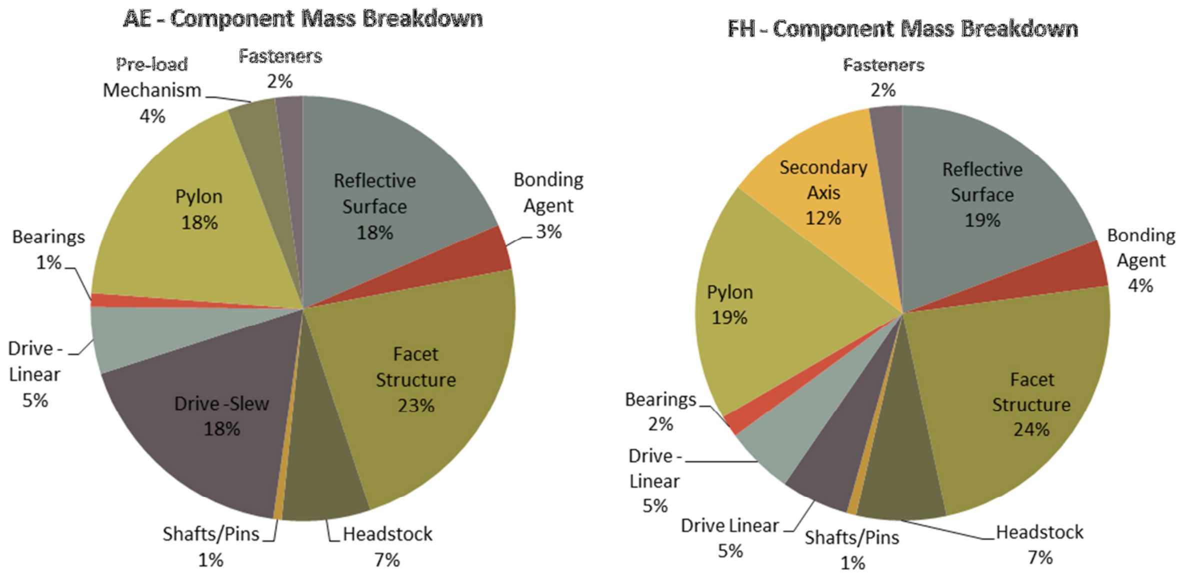

Fig. 6. Mass breakdown per heliostat component

The mass results are fairly similar for both heliostat prototypes as they have identical facets, headstocks (structural interface) and pylons. It is important to note that for both cases the total facet assembly (facet structure, bonding agent and reflective surface) equated to more than 40 % of the heliostat mass showing significant scope for stiffness optimisation and weight reduction. Fig.7 shows the percentage of commodity used per tracking mechanism.

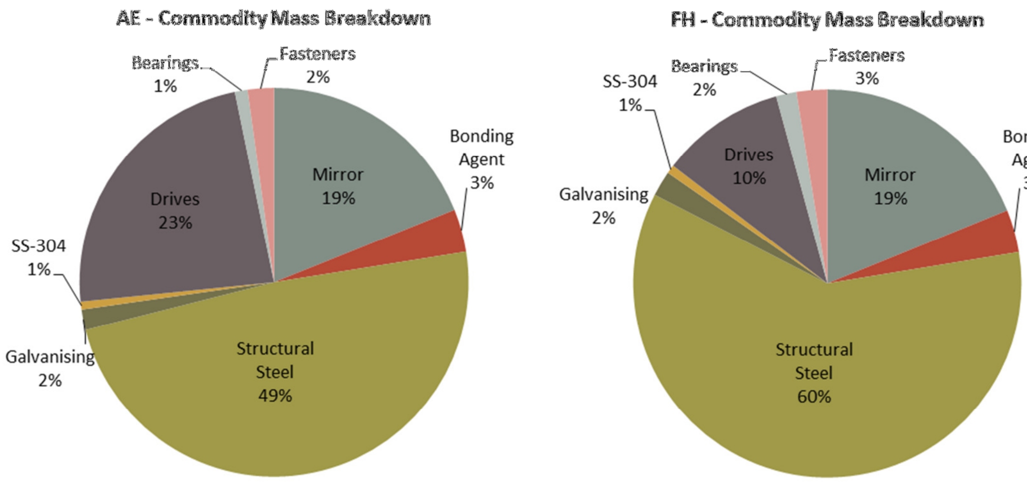

Fig. 7. Commodity mass breakdown specific to tracking mechanism

The relative proportion of heliostat mass allocated to structural steel differs by 11 percentage points; more structural steel is used in the FH design which can be accounted for by the need to include additional steel in the secondary axis structure. Furthermore the use of two linear actuators in the FH system as opposed to a single linear actuator and a slew drive results in 13 % less mass allocated to drives. A noted sensitivity which is small at this heliostat volume and scale is the increased amount of bearings required by linear actuators as each actuator tracking axis requires bearings as well as two actuator connection points per actuator. The mass allocated to the facet bonding will drop significantly in the future as a replacement bonding agent has already been sourced and early test suggest significant decrease in weight and cost. Similar to the large mass proportions allocated to the facet assembly, the quantity of structural steel in this case is an indication of scope for structural optimisation.

3.2 Material Costs

The AE mechanism and the FH mechanism cost 4 400 ZAR/ m^2 and 4 000 ZAR/ m^2 respectively. In order for central receiver systems LCOE to reach 0.10 USD/ kWh, heliostat cost goals are in the region of 120 USD/ m^2 [9]. The majority of the high cost associated with the Helio-40 project is due to the low volume. The custom steel parts were built by job-shop steel contractors outside of the university and the drives were ordered in small quantities. Due to this low volume, a large portion of the steelwork component costs are dedicated to labour overhead and profit as costing proportions differ by contractor. Cost breakdowns showing the cost/ m^2 of each component are included in Fig. 8 and Fig. 9. The steelwork contractor supplied cost breakdowns per component only, and as a result the values of the four categories shown in the graph legend for fig 8 and 9 were calculated from known component volumes and published steel and galvanising tariffs. These calculated values were then subtracted from the contractors component cost leaving the final category cost; labour, overhead and profit. In addition no cost transparency was available to directly purchased items such as drives and bearings, and as a result they were treated as a single material cost. The cost of material used shows a closer cost indication for higher volume production rates.

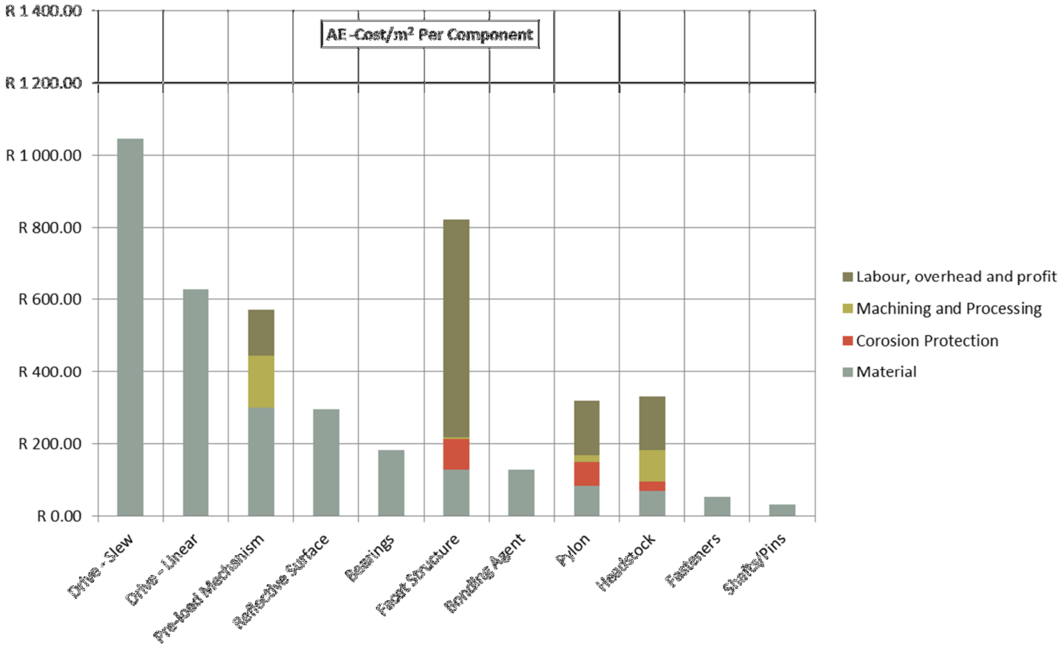

Fig. 8. Component cost breakdown, arranged in order of material cost

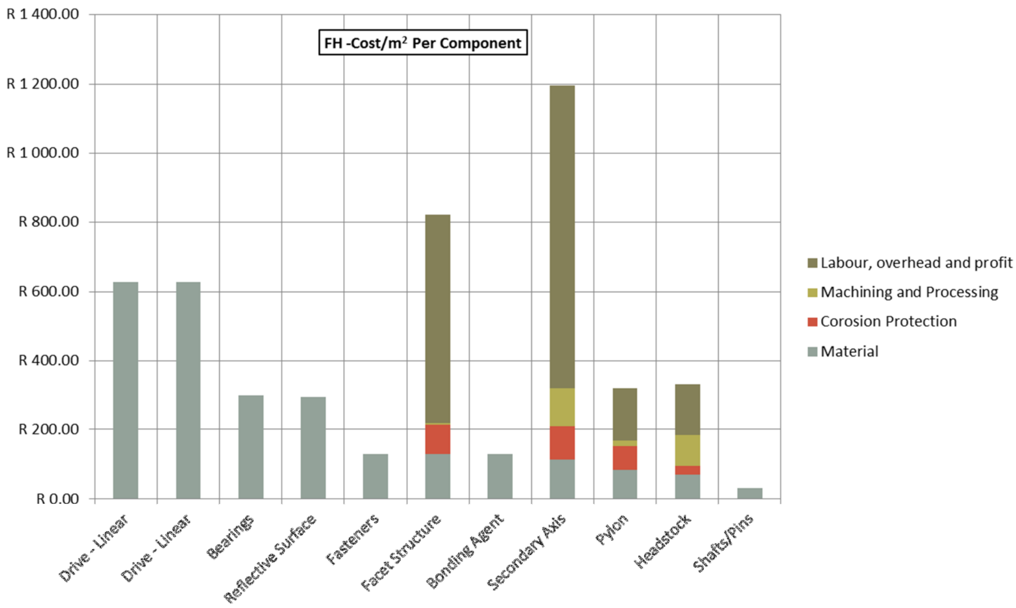

Fig. 9. Component cost breakdown, arranged in order of material cost

4 Discussion

In the case of Helio-40 the selection of a tracking mechanism has a small effect on cost, but greatly effects control, packing ratio and optical performance of the heliostat. Despite the FH tracking mechanism showing slightly lower costs per m^2 as well as greater potential for future cost reduction due to the use of linear drives, the azimuth elevation mechanism was selected for implementation into helio-40 due to its ability to rotate 360^o in the azimuth. This decision was based on safety considerations for the surrounding buildings and the need for the heliostat to stow in a southerly position in emergency stow situations.

Due to project requirements and time constraints, off-the-shelf drive systems and standard steel sections were used. These shelf items create a design and cost ceiling resulting in heliostat designs constrained by available components. Although there is currently significant scope for optimisation and cost reduction within these designs, to truly reduce long term heliostat costs, a holistic approach is required whereby the drive system, foundation, control, facet and structural supports are all designed specifically to meet the optical and economic performance outputs.

5 Conclusion

To date two working prototypes incorporating different tracking mechanisms have been designed and assembled on the solar roof laboratory. In each case the prototypes demonstrate proof of concept and successful open loop tests have been performed, showing comprehensive heliostat operation. The project is still in its infancy and significant further testing is required to quantify calibrated tracking accuracy as well as structural and optical performance. The cost results shown create a first iteration cost benchmark, provide development learning to cost, and allows for the identification of key areas of improvement and optimisation.

6 Acknowledgements

The authors would like to thank SASOL for the generous grant without which this project would not be possible. Further thanks to the Department of Mechanical and Mechatronic Engineering for aiding and facilitating this project as well as the departmental workshop staff for their valuable contribution.

7 References

[1] Detlev G. Kröger, 2012, "The Stellenbosch UNiversity Solar POwer Thermodynamic cycle," University of Stellenbosch, Stellenbosch.

[2] J. A. Peterka and R. G. Derickson, 1992, "Wind load design methods for ground based heliostats and parabolic dish collectors," Sandia National Laboratories, Springfield.

[3] Y. T. Chen, A. Kribus, B. H. Lim, C. S. Lim, K. K. Chong, J. Karni, R. Buck , A. Pfahl and T. P. Bligh, 2004, "Comparison of two sun tracking methods in the application of heliostat field," *Journal of Solar Energy Engineering,* vol. 126, pp. 1-7.

[4] P. Schramek and D. R. Mills, 2004, "Heliostats for maximum ground coverage," *Energy,* vol. 29, pp. 701-713.

[5] S. Cordes, T. C. Prosinečki and K. Wieghardt, 2012, "An approach to compeditive heliostat fields," in *Solar Paces*, Marrakesh Morocco.

[6] C. Ho, C. Ghanbari and R. Diver, 2011, "Hazard analyses of glint and glare from concentrating solar power plants," *ASMEj. Sol Energy Eng,* vol. 133, pp. 031021-1:0312012-9, 2011.

[7] A. Pfahl, 2013, "Survey of Heliostat Concepts for Cost Reduction," *Journal of Solar Energy Engineering,* vol. 136(1), ASME.DOI:10.1115/1.4024243.ISSN 0199-6231

[8] G. J. Kolb and S. A. Jones, 2007, "Heliostat Cost Reduction Study," Sandia National Laboratories, Alburquerque, NM.

[9] A. Pfahl, M. Randt, C. Holze and S. Unterschütz, 2013,"Autonomous light-weight heliostat with rim drives," *Solar Energy,* vol. 92, pp. 230-240.

[10] T. R. Mancini, 2000, "Catalog of solar heliostats," IEA-Solar Power and Chemical Energy Systems, Alburquerque, NM.

[11] G. J. Kolb, C. K. Ho, T. R. Mancini and J. A. Gary, 2011, "Power Tower Technology Roadmap and Cost Reduction Plan," Sandia National Laboritories, Albuquerque.